J Mater Sci (2011) 46:1557–1562
DOI 10.1007/s10853-010-4961-y

Wetting transition of grain boundaries in the Sn-rich part of the Sn–Bi phase diagram

C.-H. Yeh · L.-S. Chang · B. B. Straumal

Received: 18 June 2010 / Accepted: 29 September 2010 / Published online: 29 October 2010

Abstract The microstructural evolution of tin-rich Sn–Bi alloys after the grain boundary wetting phase transition in the (liquid + β-Sn) two-phase region of the Sn–Bi phase diagram was investigated. Three Sn–Bi alloys with 30.6, 23, and 10 wt% Bi were annealed between 139 and 215 °C for 24 h. The micrographs of Sn–Bi alloys reveal that the small amount of liquid phase prevented the grain boundary wetting transition to occur during annealing close to the solidus line. The melted area of the grain boundary triple junctions and grain boundaries increased with increasing the annealing temperature. When the amount of liquid phase exceeded 34 wt% during annealing, increasing temperature has not affected the wetting behavior of grain boundaries noticeably and led only to the increase of the amount of liquid phase among solid grains in the microstructure. The XRD results show that the phase structure and crystallinity remained unchanged after quenching from various annealing temperatures.

Introduction

Polycrystalline materials contain various interfaces such as grain and interphase boundaries. These interfaces can undergo various transformations with changing temperature. When liquid melt appears among the solid crystals during heat treatment, it usually changes the microstructure and affects many properties of polycrystalline materials. Frequently, the grain boundary (GB) wetting phase transition occurs in metals and ceramics [1–3]. The grain boundary wetting transition is a complex phenomenon involving thermodynamic, kinetic, and structural features of the GB, solid/liquid interface, and various diffusion paths [4]. The occurrence of GB wetting transition depends on the grain boundary energy, σ_{GB}. Consider the liquid (melted) phase in the contact with a solid phase containing a boundary between the misoriented grains. If the σ_{GB} is lower than $2\sigma_{SL}$, where σ_{SL} is the energy of the solid/liquid interphase boundary, the GB is incompletely wetted and the dihedral contact angle $\theta > 0°$. But if σ_{GB} is higher than $2\sigma_{SL}$, the GB is completely wetted by the liquid phase and $\theta = 0°$. The $2\sigma_{SL}$ decreases with increasing temperature faster than σ_{GB} because the solid–liquid interface exhibits higher excess entropy than the grain boundary. If the temperature dependences σ_{GB} and $2\sigma_{SL}$ intersect, the GB wetting transition occurs at the temperature T_w of their intersection. The dihedral contact angle, θ, decreases down to zero gradually when temperature increases to T_w. In polycrystals, many GBs have different free energies and the wetting temperatures (T_w) of the GBs also differ. Therefore, the maximal $T_{w,max}$ and minimal wetting temperature $T_{w,min}$ can be found for GBs with minimal and maximal energy, respectively [5]. When the temperature increases from $T_{w,min}$ to $T_{w,max}$, the fraction of wetted GBs increases from 0% to 100%. The GB wetting transition has been studied in several alloy systems [6–8] and its influence on the properties of polycrystals has also been demonstrated, for example ionic conductivity, thermal conductivity, and liquid metal embrittlement [9–11].

C.-H. Yeh · L.-S. Chang (✉)
Department of Materials Science and Engineering, National Chung Hsing University, 40227 Taichung, Taiwan, ROC
e-mail: lschang@dragon.nchu.edu.tw

B. B. Straumal
Institute of Solid State Physics, Russian Academy of Sciences, Chernogolovka, Moscow District 142432, Russia

B. B. Straumal
Max-Planck-Institut für Metallforschung, Heisenbergstrasse 3, 70569 Stuttgart, Germany

The liquid metals with low melting point such as Pb, Sn, In, and Bi play an important role in soldering in microlectronics, thermal interface joining, or heat transfer by liquid metals in nuclear reactors, etc. [12, 13]. In some of these applications, an important factor for lifetime of the solid is the GB wetting and penetration by the liquid melt. Some Sn-based alloys like Sn–Zn [14–16], Sn–Al [7, 17], Al–Sn–Ga [18], Sn–In [19] etc. were already investigated. The Sn–Bi alloy is frequently applied to replace the Sn–Pb alloy in soldering as well. Simultaneously, bismuth has a higher melting temperature than tin. It makes difficult the investigation of the GB wetting phase transition in the Sn-rich Sn–Bi alloys alloys by the individual grain boundary method. In this study, the wetting behavior of grain boundaries in polycrystalline Sn-rich Sn–Bi alloys at various temperatures in the (liquid + β-Sn) two-phase region of the Sn–Bi phase diagram was investigated.

Experimental

Three Sn–Bi alloys with 30.6, 23, and 10 wt% Bi were prepared by weighing out the appropriate amount of Sn (99.999%) and Bi (99.999%) slugs, sealing into quartz tubes in an argon atmosphere, and annealed in the furnace at 350 °C until the mixture was fully melted. These alloy sticks were homogenized for 24 h at 100 °C and then were sliced into several specimens. In order to obtain uniform microstructures, the specimens were plastically deformed by light hammer blows and annealed for 20 h at 120 °C.

These Sn–Bi specimens were annealed between 139 and 220 °C for 24 h to approach the phase equilibrium and quenched into salt-saturated ice water at −10 °C and into liquid nitrogen. The deviation of annealing temperatures was controlled within ±1 °C. After annealing, specimens were mechanically ground and polished using 0.3 and 0.05 μm Al_2O_3 powder. The Sn–Bi specimens were etched in a dilute solution of 2% HCl, 5% HNO_3, and 93% H_2O for 15 s to reveal the metallographic microstructure. The microstructures of specimens were observed using an optical microscope (OM, HM-2000, Bao-I Technology Corporation) equipped with a digital 7.1 Mpix UCAM camera and a field-emission scanning electron microscope (FESEM, JSM-6700F, JEOL Instrument). The portion of completely wetted GBs was counted using software for quantitative metallography. The quantification of the wetted GBs by the OM analysis was performed adopting the following criterion: every GB was considered to be wetted only when a continuous layer had covered the whole (visible part of the) GB; if such a layer appeared to be interrupted, the GB was regarded as a non-wetted (incomplete wetted) GB. Over one hundred GBs were analyzed at each annealing temperature. An X-ray diffractometer (XRD, Model MAC SCIENCE MXP-III, Bruker Corporation) was used to identify phases of the samples. The XRD parameters were acquired in the diffraction angle interval 2θ between 20° and 80° with a sampling width of 0.02° and scanning speed of 2°/min.

Results and discussion

Tin–bismuth alloys have low melting points and the eutectic temperature is 139 °C. The Sn–Bi alloys with Bi content between 0 and 57 wt% have melting points in the range 139–232 °C and an extensive (liquid + β-Sn) two-phase region (Fig. 1). The Sn–23 wt% Bi specimens were annealed for 24 h between 141 and 182 °C. Figure 2 shows the optical micrographs of annealed Sn–23 wt% Bi specimens, at a low magnification. After Sn–23 wt% Bi specimens were annealed below 146 °C, the GB wetting was not clearly observed in the light micrographs. However, the backscattered electron images reveal that the Bi atoms dissolved in the Sn matrix and then gradually diffused to the grain boundaries during annealing at 146 °C (Fig. 3). When the Sn–23 wt% Bi specimen was annealed at 152 °C, the phenomenon of GB wetting transition became more distinct. It can be seen that the most grain boundaries were already wetted by the liquid phase and the liquid phase penetrated among some solid grains to form a liquid layer. The amount of completely wetted GBs increased gradually and the liquid layers expanded their thickness with increasing annealing temperature. Almost all grain boundaries were substituted by a liquid layer and only few GBs with low energy were not completely wetted after annealing at 182 °C. Upon annealing at 182 °C, the number of solid grains decreased in comparison with lower temperature and the liquid layer transforms into a large

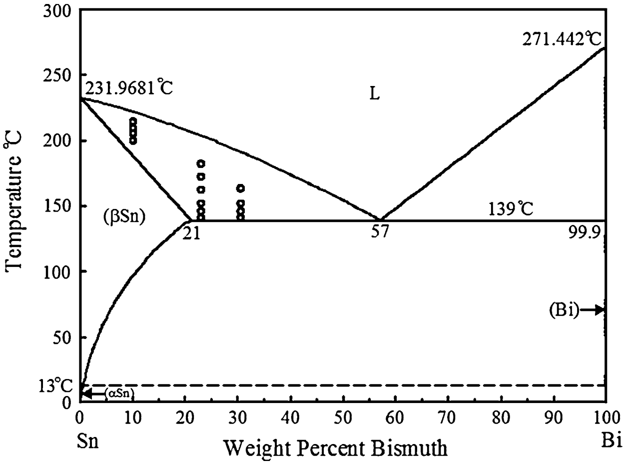

Fig. 1 The Sn–Bi bulk phase diagram [20]. Points show the compositions of the studied alloys and annealing temperatures

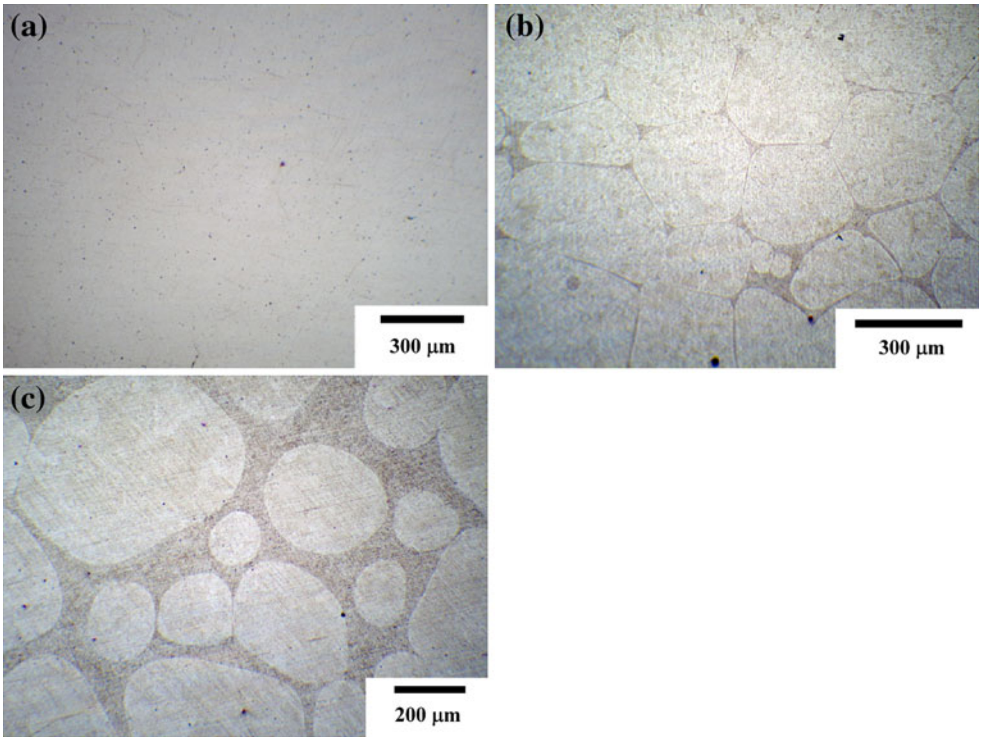

Fig. 2 Optical micrographs of the Sn–23 wt% Bi specimens annealed for 24 h at **a** 141 °C, **b** 152 °C, **c** 182 °C

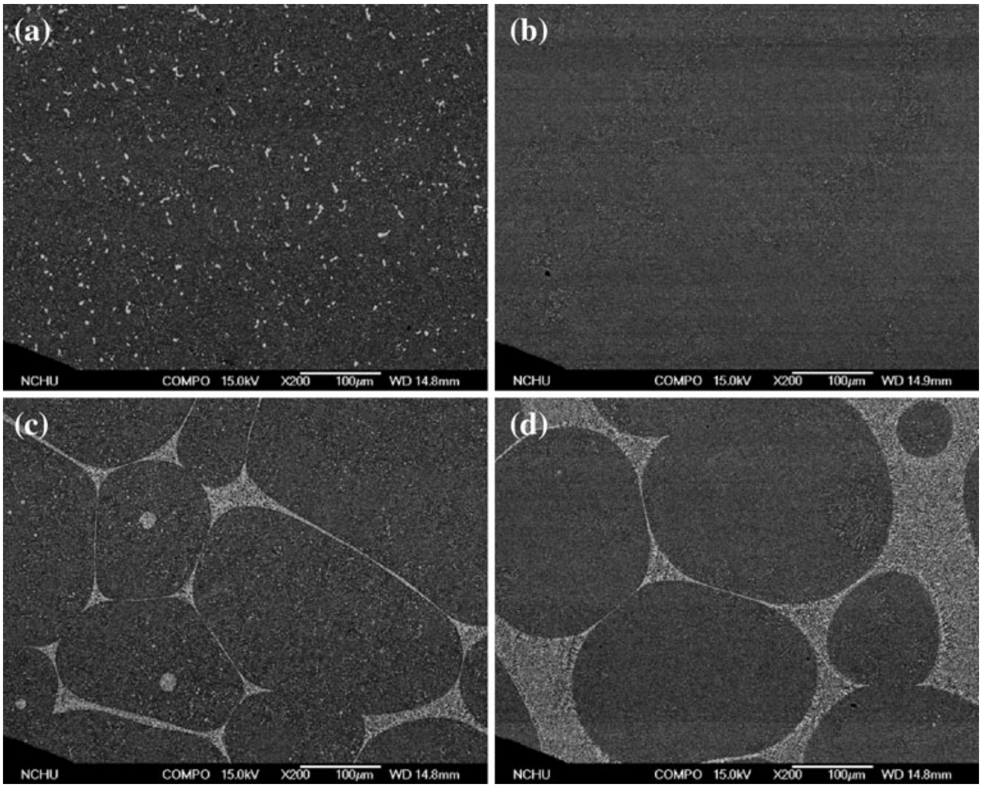

Fig. 3 BEI images of the **a** as-prepared Sn–23 wt% Bi specimens and after annealings for 24 h at **b** 146 °C, **c** 152 °C, and **d** 182 °C. β-Sn solid grains appear *black*; GB wetting layers appear *white*

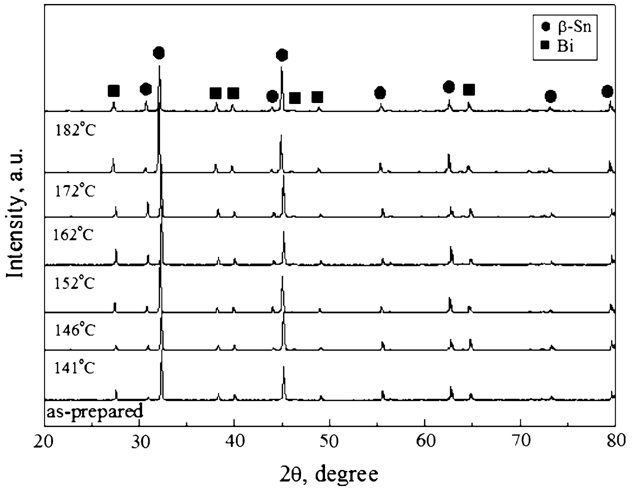

Fig. 4 XRD patterns of the as-prepared Sn–23 wt% Bi alloy and after annealing at 141–182 °C

liquid phase region among the grains. Figure 4 shows the XRD results for the Sn–23 wt% Bi via annealing at 141 °C to 182 °C. During quenching, the liquid phase underwent eutectic transformation and became a mixture of *β*-Sn and Bi solid phases. The position and intensity of XRD peaks have no apparent differences after quenching from different temperatures.

Figure 5 shows the microstructure of Sn–30.6 wt% Bi specimens annealed for 24 h at 141 and 152 °C. Numerous grain boundaries of the annealed Sn–30.6 wt% Bi specimen were completely wetted by the liquid phase during annealing at 141 °C, just 2 °C above the eutectic temperature. Comparing the micrographs of Sn–23 wt% Bi and Sn–30.6 wt% Bi specimens annealed at 141 °C, we observe that the small amount of liquid phase (<10 wt%) and the larger atomic volume of Bi element made it difficult for the Bi atoms to diffuse into the grain boundaries in the Sn matrix. However, the Bi contents of *β*-Sn solid phase and liquid phase decreased and the fraction of liquid phase increased with temperature as the $Sn_{77}Bi_{23}$ alloy annealed in the (liquid + *β*-Sn) two-phase region. The Bi content of liquid phase in annealed $Sn_{77}Bi_{23}$ alloy decreased with increasing temperature could promote the liquid phase to appear in the GB regions. The liquid layers among solid grains can provide Bi atoms with the rapid diffusion paths. Therefore, the amount of liquid phase can affect the kinetics of GB wetting transition in the Sn-rich Sn–Bi alloys alloy. When the Sn–23 wt% Bi specimens were annealed at 152 °C, at which the amount of liquid phase was about 15 wt%, the GB wetting can be clearly observed. Figure 6 shows the microstructures of annealed Sn–10 wt% Bi alloy. Almost all grain boundaries were occupied by the liquid phase layers during annealing upon 200 °C. As the annealing temperature increased close to the liquidus temperature, the number of solid grains decreased gradually and the liquid phase became the major phase in the structure.

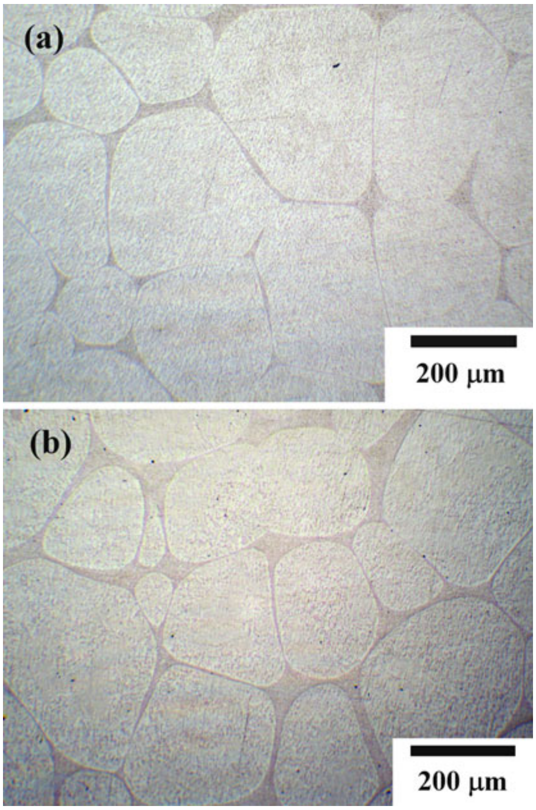

Fig. 5 Optical micrographs of the Sn–30.6 wt% Bi specimens annealed for 24 h at **a** 141 °C and **b** 152 °C

Figure 7 shows the statistical results for the completely wetted GBs of Sn–Bi alloys with 30.6, 23, and 10 wt% Bi at various annealing temperatures. The fraction of completely wetted GBs of Sn–23 wt% Bi and Sn–30.6 wt% Bi alloys depends on the annealing temperature. When the Sn–23 wt% Bi specimens were annealed between 141 and 182 °C, the fraction of completely covered GBs increased from 0% to 94% with increasing annealing temperature. The Sn–30.6 wt% Bi specimens were annealed between 141 and 163 °C and the fraction of wetted GBs gradually increased from 80% to 96% with increasing temperature. The proportion, 80%, of the GBs that are completely wetted by annealing at 141 °C, which is slightly above the eutectic temperature is such that the minimal wetting temperature, $T_{w,min}$, cannot be found within the region of coexistence of the two (liquid + *β*-Sn) phases in the Sn–Bi phase diagram. The fraction of completely wetted GBs of Sn–10 wt% Bi alloys is between 93% and 95% after annealing between 200 and 214 °C for 24 h. A few grain boundaries with low energy were not completely wetted by liquid phase as the annealing temperature was close to the liquidus temperature. Simultaneously, the statistical results

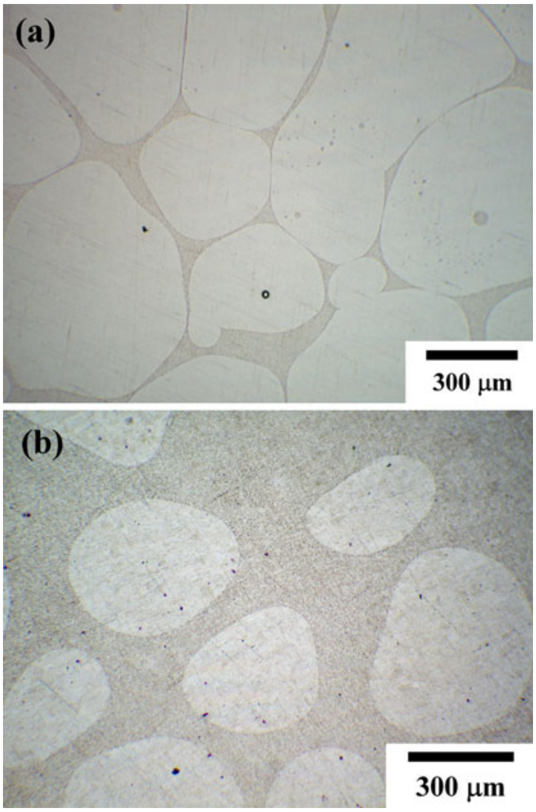

Fig. 6 Optical micrographs of the Sn–10 wt% Bi specimens annealed for 24 h at **a** 200 °C and **b** 214 °C

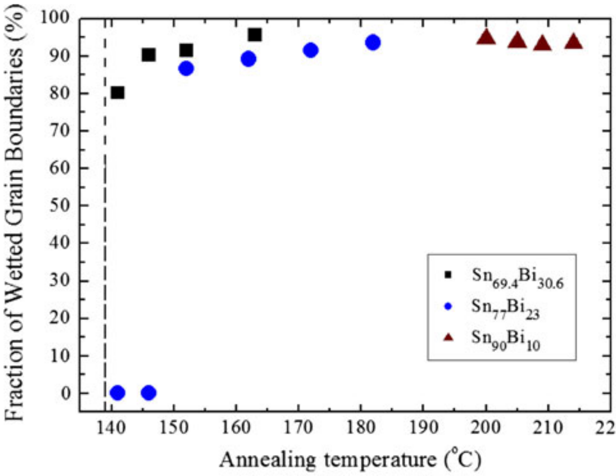

Fig. 7 Fraction of the completely wetted GBs in dependence on the annealing temperature for the Sn-rich Sn–Bi alloys

for the completely wetted GBs of Sn–Bi alloys with 25 and 34 wt% of the liquid phase are also shown in Fig. 8. The fraction of completely wetted GBs increases with the annealing temperature at 25 wt% of the liquid phase. However, for 34 wt% of the liquid phase, the fraction of completely wetted GBs are between 91% and 94% upon 151 °C and the liquid phase occupied the most regions among the grains gradually. Therefore, it reveals that increasing temperature has not affected the wetting behavior of grain boundaries noticeably, when the liquid content was 34 wt% and annealing was above 151 °C in Sn-rich Bi alloys.

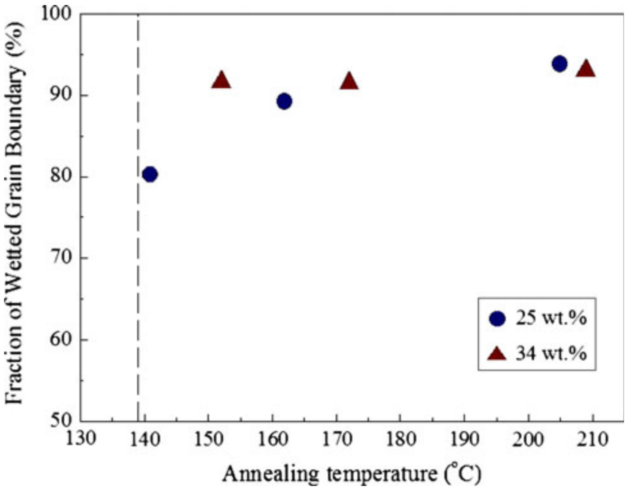

Fig. 8 Fraction of the completely wetted GBs in dependence on the annealing temperature for the liquid phase content in the Sn-rich Sn–Bi alloys of 25 wt% and 34 wt%

Conclusions

Three Sn-rich Sn–Bi alloys with 30.6, 23, and 10 wt% Bi were annealed in the (liquid + β-Sn) two-phase region of the Sn–Bi phase diagram to investigate their microstructural evolution after the GB wetting phase transition. The melt gradually wetted the grain boundaries with increasing annealing temperature in Sn–23 wt% Bi and Sn–30.6 wt% Bi alloys. In the Sn–23 wt% Bi alloy, the fraction of wetted GBs gradually increased from 0% to 94% as the temperature increased from 141 and 182 °C. In the Sn–30.6 wt% Bi alloy, the fraction of wetted GBs gradually increased from 80% to 96% as temperature increased from 141 to 163 °C. The small amount of liquid phase (<10 wt%) can delay the GB wetting transition during annealing above the eutectic temperature. When the amount of liquid phase exceeds 34 wt% during annealing, increasing temperature did not affect the wetting behavior of grain boundaries noticeably and led only to the increase of the amount of liquid phase among solid grains in the microstructure. The XRD results show that the phase structure and crystallinity remained unchanged after quenching from various annealing temperatures.

Acknowledgements This work was financially supported by the Russian Foundation for Basic Research under the contract 05-03-90578 and National Scientific Council of Taiwan under the contracts NSC 96-2218-E-005-015.

References

1. Straumal BB, Zieba P, Gust W (2001) Int J Inorg Mater 3:1113
2. Clarke DR (1999) Mater Sci Forum 294–296:1
3. Belousov VV (2005) J Mater Sci 40:2361. doi:10.1007/s10853-005-1959-y
4. Lojkowski W, Rabkin E, Straumal B, Shvindlerman LS, Gust W (1998) Defect Diffus Forum 156:163
5. Straumal B, Baretzky B (2004) Interface Sci 12:147
6. Straumal BB, López GA, Mittemeijer EJ, Gust W, Zhilyaev AP (2003) Defect Diffus Forum 216–217:307
7. Straumal B, Molodov D, Gust W (1996) Mater Sci Forum 207–209:437
8. Straumal BB, Gornakova AS, Kogtenkova OA, Protasova SG, Sursaeva VG, Baretzky B (2008) Phys Rev B 78:1
9. Pezzotti G, Nakahira A, Tajika M (2000) J Eur Ceram Soc 20:1319
10. Fedorov SV, Belousov VV (2009) Russ J Electrochem 45:573
11. Ludwig W, Pereiro-López E, Bellet D (2005) Acta Mater 53:151
12. Chriaštel J, Ožvold M (2008) J Alloy Compd 457:323
13. Jones WK, Liu YQ, Shah M (1997) In: 3rd international symposium on advanced packaging materials, p 64
14. Gornakova AS, Straumal BB, Tsurekawa S, Chang L-S, Nekrasov AN (2009) Rev Adv Mater Sci 21:18
15. Murashov V, Straumal B, Protsenko P (2006) Defect Diffus Forum 249:235
16. Straumal BB, Gust W, Watanabe T (1999) Mater Sci Forum 294–296:411
17. Straumal B, Gust W, Molodov D (1994) J Phase Equilib 15:386
18. Straumal B, Risser S, Sursaeva V, Chenal B, Gust W (1995) J Phys IV C7:233
19. Yeh C-H, Chang L-S, Straumal B (2006) Defect Diffus Forum 258–260:491
20. Massalski TB, Okamoto H, Subramanian PR, Kacprzak L (1990) Binary alloy phase diagrams. ASM International, Materials Park, OH